01 Aug 1997

Lumped-Element Sections for Modeling Coupling Between High-Speed Digital and I/O Lines

Wei Cui

Hao Shi

Xiao Luo

Fei Sha

et. al. For a complete list of authors, see https://scholarsmine.mst.edu/ele_comeng_facwork/1110

Recommended Citation

Lumped-element Sections for Modeling Coupling Between High-Speed Digital and I/O Lines

W. Cui, H. Shi, X. Luo, F. Sha*, J.L. Drewniak, T.P. Van Doren and T. Anderson**
Electromagnetic Compatibility Laboratory
University of Missouri-Rolla
Rolla, MO 65401

* Northern Jiao Tong University
EMC Research Section
Beijing 100044, P.R.China

** HP-EEsof Division
Hewlett-Packard Co.
Santa Rosa, CA 95403

Abstract: Lumped-element sections are used for modeling coupling between high-speed digital and I/O lines on printed circuit boards (PCBs) in this paper. Radiated electromagnetic interference (EMI) is investigated when the I/O line going off the board is driven as an unintentional, but effective antenna. Simulated results are compared with measurements for coupled lines. A suitable number of lumped-element sections for modeling is chosen based on the line length and the highest frequency of interest.

I. INTRODUCTION

As the speed of digital designs continues to increase, unintentional radiation from cables attached to PCBs becomes problematic. For clock speeds less than 50 MHz, a typical 1 m cable attached to a PCB is an electrically short antenna for all but very high harmonics. Since the magnitude of the input impedance of an electrically short antenna exceeds 500 Ω and is almost entirely reactive, an electrically short cable driven against a PCB or conducting enclosure is not easily driven by a noise source of moderate impedance. However, as clock frequencies exceed several hundred megahertz, nearly all cables attached to a PCB will be of resonant dimensions for low-order harmonics. Resonant dipole-type EMI antennas typically have an input impedance on the order of 100 Ω, and can be effectively driven by low-impedance noise sources to result in an EMI problem. Coupling between a high-speed digital line and an adjacent I/O line can provide an unintentional source to drive this antenna. Even a few centimeters of common length for two closely spaced lines can cause strong coupling and a potential EMI problem. Quantifying and modeling the coupling between two transmission lines or multiconductor transmission lines is essential to analyze and evaluate this class of EMI problems. Simple and reliable modeling techniques are required at the design stage to estimate EMI and minimize the noise coupling to I/O lines on the PCB. As digital designs become more dense, flexibility in trace routing is reduced. Adherence to simple design maxims for avoiding adjacent segments of an I/O line and a high-speed digital line becomes more difficult. A means for estimating EMI at the design stage is desirable to maintain routing flexibility while minimizing EMI risk.

The three essential components for estimating EMI resulting from coupling to I/O lines are suitable source and load models, a coupled transmission-line model, and an EMI antenna model. Of particular interest at this stage are models for the coupled transmission lines, and the EMI antenna. Two approaches have been previously pursued for modeling coupled transmission-lines. One technique is to decouple the lines in the frequency domain by modal decomposition [1]. Transient analysis of a lossy line has also been reported [2]. A second method is to divide the coupled line into a number of lumped-element sections [3]. Although the lumped-element section approach is an approximation to the distributed transmission line with some artifacts, this modeling is easier to implement, and compatible with general-purpose circuit simulation tools such as SPICE. Moreover, the frequency-dependent line loss can be easily incorporated into a lumped-element model, and IBIS device models, terminations, and filtering can also be easily integrated.

An approach for modeling the coupling using cascaded lumped-element sections is presented herein together with a simple antenna model for determining a worst-case EMI estimate. This modeling method can be used to provide an estimate of EMI due to coupling to I/O lines in high-speed designs.

II. LUMPED-ELEMENT MODELING OF COUPLED TRANSMISSION LINES

A lumped-element circuit model is typically used to approximate a transmission line when the line is electrically short. As the frequency becomes higher, a lumped-element model can still provide adequate results for coupling if a sufficient number of lumped sections are employed. A commonly used broad maxim is five lumped-element sections per wavelength at the highest frequency of interest [3]. The lumped-element sections can be in the form of π, T, Γ or backward Γ models [3][4]. The parameters of each section are the per-unit-length quantities times the section length. A coupled π-section, shown in Figure 1, with element parameters R^i, G^i, L^i, C^i, $L_m{}^i$ and $C_m{}^i$ was used in this study.
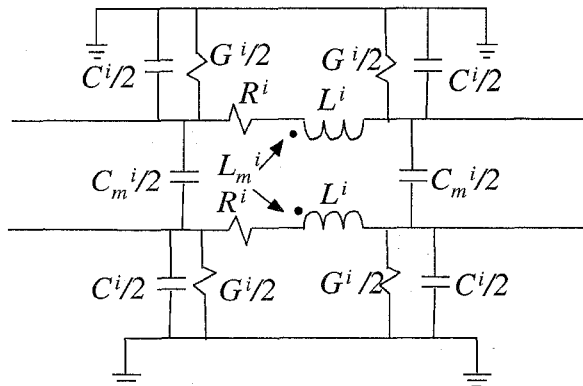

Figure 1. A coupled lumped-element π-section for modeling coupled transmission lines.

The values of elements for the ith section are

$$R^i = \frac{rd}{N} \quad (1\text{-}a), \qquad G^i = \frac{gd}{N} \quad (1\text{-}b),$$

$$L^i = \frac{ld}{N} \quad (1\text{-}c), \qquad C^i = \frac{cd}{N} \quad (1\text{-}d),$$

$$L_m{}^i = \frac{l_m d}{N} \quad (1\text{-}e), \qquad C_m{}^i = \frac{c_m d}{N} \quad (1\text{-}f),$$

where r, g, l and c are the self per-unit-length parameters of the transmission line, l_m and c_m are the per-unit-length mutual parameters, d is the line length, and N is the total number of sections used for modeling the line.

The choice of the number of cascaded lumped-element sections is a key factor in the accuracy of this approach for modeling transmission lines. In general, each section of the lumped-element model must be electrically short at the highest frequency of interest. However, in order to achieve higher accuracy, other criteria for the number of sections have been suggested [3]. Previously published error criteria are based on lumped-element sections for modeling a single line, and include errors in the characteristic impedance, natural resonance frequencies, and [ABCD] matrix coefficients. For

example, the criteria based on characteristic impedance requires a number of sections N such that

$$N \geq 14.14 \frac{d}{\lambda} , \qquad (2)$$

where d is the length of the modeled line, and λ is the wavelength of the highest frequency of interest, to achieve an error of 2.5% or less. The published error criteria for single line sections can also be applied to coupled lines using modal decomposition and applying the criteria to each mode.

Useful insight can be gained by defining a simple error based on |S21| between the driven line, and the coupled I/O line going off the board as

$$\varepsilon = \frac{|\,|S21^N| - |S21^{\text{txline}}|\,|}{|S21^{\text{txline}}|} \times 100\% , \qquad (3)$$

where |S21$^{\text{txline}}$| is from the solution for coupling between two transmission lines using the transmission-line equations and modal decomposition. A disadvantage of this error definition is that it is a function of the terminations on both the driven and coupled lines. The error defined in Equation (3) is plotted in Figure 2 for the case of two coupled lossless transmission lines with the driven line and far-end of the coupled line terminated in open circuits. Although the error increases abruptly at certain frequencies, these frequencies correspond to resonances in the coupled lines at which the coupling is a minimum. For example, the first minimum in |S21| in Figure 6(a) occurs at approximately 180 MHz ($\lambda_{\text{FR-4}} \approx 80$ cm) and the ratio of the coupling length d=17.8 cm to the wavelength is approximately 0.22.
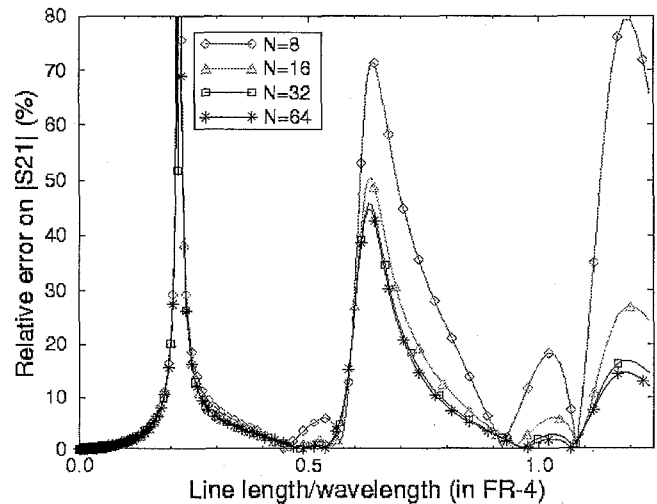

Figure 2. Relative error on |S21| for N= 8, 16, 32 and 64.

The error shown in Figure 2 converges to its final value, i.e., no further changes with additional sections, with approximately 64 sections in the frequency range shown (0< d/λ < 1.25). The convergence is similar for other loading conditions of the driven and coupled lines. An approximate

number of sections per normalized length of coupled transmission lines is then

$$N \geq 50\frac{d}{\lambda} \quad . \tag{4}$$

Although this is a factor of ten greater than typically suggested for single lines [3], and three times that of Equation (2), good comparison of the simulated and experimental results (shown in the next section) requires a finer discretization than five sections per wavelength over the coupled segments.

III. DETERMINATION OF LINE PARAMETERS

There are several approaches for determining the per-unit-length parameters of a transmission line. For certain conductor configurations in a homogeneous medium, the per-unit-length parameters can be calculated in closed-form from cross-sectional dimensions [5]. However, for microstrip lines, striplines and other PCB traces, in which closed-form solutions are not available, empirical expressions are often used [6][7]. For more complex configurations characteristic of PCB geometries, such as asymmetric microstrip or stripline where the coupled lines do not lie on the same layer, the per-unit-length parameters can be determined by numerical cross-section analysis commonly employed in signal integrity tools. Here, an experimental method is used to determine the self and mutual capacitance and inductance of a transmission line. The self capacitance and inductance are also calculated with a cross-section analysis tool LineSim Pro for comparison.

The self capacitance and inductance per-unit-length are related to the characteristic impedance of the transmission line, as well as the speed of the signal traveling down the line. The per-unit-length parameters can be determined by measuring the characteristic impedance, and the time of flight (or delay time) of a step signal. The wavespeed v, and characteristic impedance Z_o are related to l and c as

$$v = \frac{c_o}{\sqrt{\varepsilon_r}} = \frac{1}{\sqrt{lc}} = \frac{d}{t_d}, \tag{5}$$

$$Z_o = \sqrt{\frac{l}{c}}, \tag{6}$$

where d is line length, t_d is the time of flight, and ε_r is the relative dielectric constant of the PCB. The values of l and c can be calculated from the measured values of d, Z_o and t_d, while Z_o and t_d can be measured with a time-domain reflectometer (TDR), and d can be obtained from layout diagrams or a simple length measurement. Equation (5) also gives a good estimate of ε_r for measured values of t_d and d. This value is the relative dielectric constant for a measurement with a stripline configuration, or effective relative dielectric constant for a microstrip line.

Mutual capacitance and inductance can be determined experimentally as well. In the low-frequency range where the transmission lines are electrically short, either capacitive or

inductive coupling dominates for an open or short termination, respectively, of the driven line [4]. In either case, the coupling is proportional to the mutual parameters, and the mutual capacitance and inductance can be determined from S21 measurements. An equivalent circuit for this measurement is shown in Figure 3.
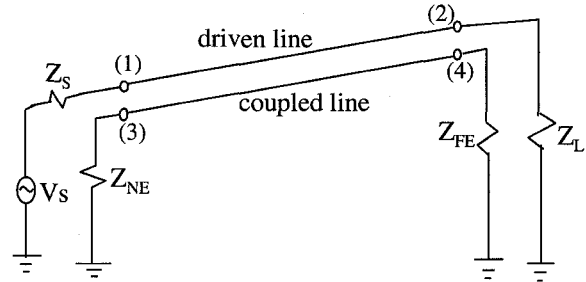

Figure 3. Two coupled transmission lines.

If the load of the driven line is shorted ($Z_L=0$), mutual inductive coupling is dominant at low frequencies. If the near-end load of the coupled line is also shorted ($Z_{NE}=0$), then

$$|\,S41\,| = \frac{|V_4^-|}{|V_1^+|} = \frac{|V_{FE}|}{|V_s/2|} \approx \frac{|j\omega L_m I_1|}{|I_1 Z_s|/2} = \frac{2\omega L_m}{Z_s}, \tag{7}$$

where Z_s is the 50 Ω source impedance of the network analyzer. From Equation (7), $|S41|$ is proportional to mutual inductance, and increases with frequency by 20 dB/decade. Likewise, the mutual capacitance can be determined with S41 measurements by open circuiting the load of the driven line and the near-end load of the coupled line. In this case, mutual capacitive coupling is dominant at low frequencies. For $Z_L=Z_{NE}=\infty$,

$$|\,S41\,| = \frac{|V_4^-|}{|V_1^+|} = \frac{|V_{FE}|}{|V_s/2|}$$

$$= \frac{2|Z_{FE}|}{|Z_s + Z_{FE} + 1/j\omega C_m|} \approx 2\omega Z_{FE} C_m, \tag{8}$$

where Z_{FE} is the 50 Ω impedance of Port 2 of the network analyzer. Again, $|S41|$ increases with frequency by 20 dB/decade.

IV. SIMULATED AND EXPERIMENTAL RESULTS

Simulations and measurements of coupling to I/O lines were made to test the lumped-element section modeling for coupled microstrip lines. A special 10-layer test board with a FR-4 dielectric substrate was used for this study. The layer stackup from top to bottom was SIG1-GND-SIG2-GND-SIG3-SIG4-GND-SIG5-GND-SIG6, where SIG is a signal conductor plane. The trace cross-sectional geometry is shown for the coupled microstrip in Figure 4.

The dielectric constant of the FR-4 substrate, and the line self parameters were determined experimentally through time of flight and impedance measurements with a Tektronix 11801B
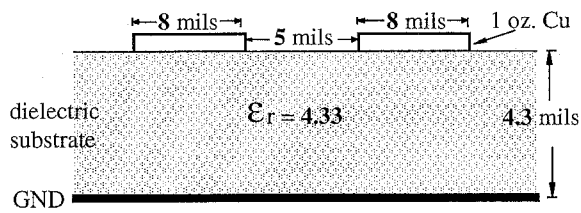
262

Figure 4. Cross-section geometry of the coupled lines studied.

TDR. Since the 17.8 cm lines used in this investigation were relatively long given the 10 *ps* rise-time of the source, time-of-flight measurements gave a reasonably good measurement of line characteristic impedance and ε_r. The measured and simulated results for the line self parameters are compared in Table 1. The simulated results were computed with LineSim Pro, a signal integrity and circuit analysis CAD tool that includes line cross-sectional analysis for self parameters. The line thickness was included in the LineSim Pro calculation.

Table 1. The per-unit-length parameters for two coupled microstrip lines

Per-unit-length parameters	Experimental Data	Simulated Result
self inductance *l* (nH/m)	280	263.4
self capacitance *c* (pF/m)	135	133
mutual inductance l_m (nH/m)	70.79	N/A
mutual capacitance c_m (pF/m)	33.71	N/A

Simulated near-end and far-end coupling with different impedances at the loads in the driven line and the coupled line were compared with measurements for the microstrip geometry. The |S21| was measured between the driven and coupled lines using an HP8753C network analyzer. SMA-connectors were used on the board, and the network analyzer calibration did not include the test connectors. The coupled lines were modeled with lossless π-sections. The segments of the coupled line l_2 shown in Figure 5 were modeled with N=64 π-sections, while l_1 and l_3 are modeled as ideal lossless transmission lines.

The measured and modeled results for near-end and far-end coupling with the driven line short and open circuited are compared in Figure 6. In general, the agreement is reasonably good for the frequency range studied to 1 GHz, in particular for the open-circuit load cases in Figures 6 (a) and (b). There are some discrepancies for the short circuit loading cases, in particular in the resonant frequencies and amplitudes. The discrepancies could result in part from the additional inductance in the shorted loads due to the connectors that
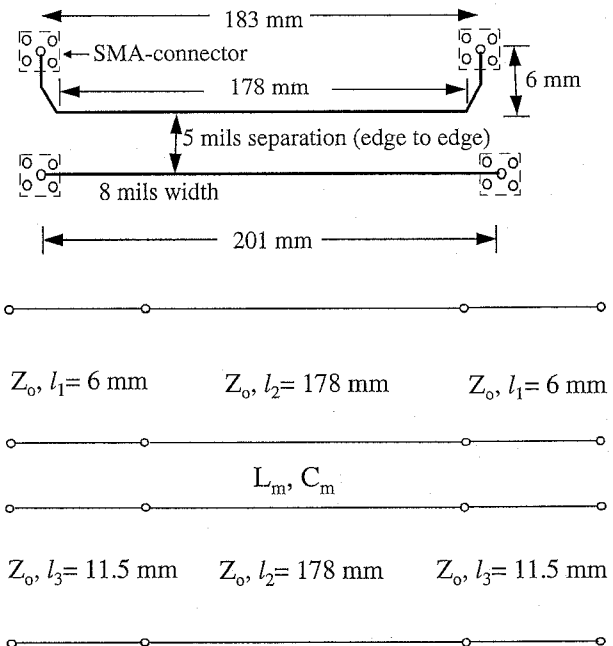

Figure 5. Coupled line dimensions and transmission line modeling.

might impact the effective electrical length. Neglecting the conductor loss may also contribute to the difference in amplitude, particularly at the higher frequencies, which would affect the shorted cases. The discrepancy for the short-circuit loading cases below 2 MHz may be a result of the finite conductor resistance as well.

It is interesting to note for this particular geometry that the coupling at low frequencies is approximately the same for the capacitive and inductive cases. Using Equations (7) and (8),

$$\frac{|S21|_{L_m}}{|S21|_{C_m}} = \frac{L_m}{50^2 C_m} . \tag{9}$$

For the values of l_m and c_m in Table 1, the ratio is approximately -1.5 dB.

V. AN EMI ESTIMATE FOR COUPLING TO I/O LINES

A cable attached to an I/O line and going off the board can be driven against the PCB ground or chassis as a dipole-type antenna. Noise coupled to the I/O line from a clock or high-speed data line results in a common-mode current on this EMI antenna, and radiation is emitted. The cable in the present case is driven against the PCB ground that comprises the other portion of the dipole-type antenna. At higher order harmonics, this EMI antenna has a low impedance that can result in significant common-mode current and an EMI problem. For the purpose of determining the common-mode current and estimating EMI, the dipole-type antenna is considered as a
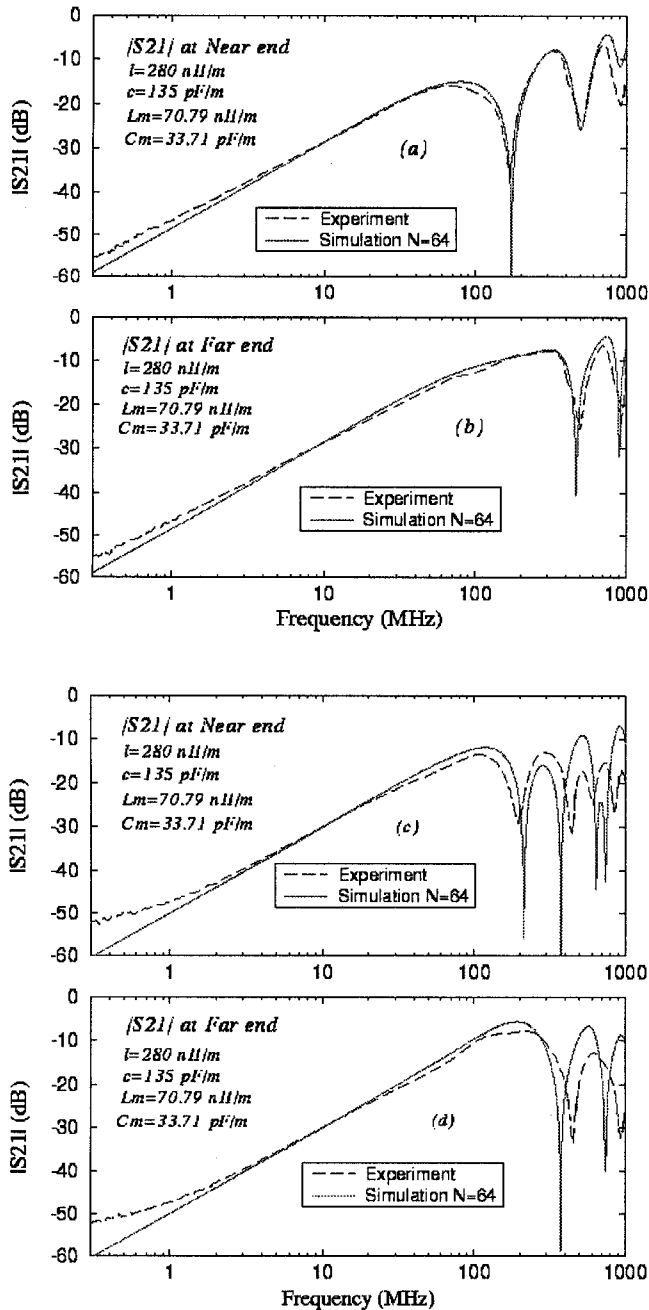
Figure 6. Experimental and simulated result of coupling between microstrip lines with
(a) $Z_L=Z_{FE}=\infty, Z_s=Z_{NE}=50\ \Omega$;
(b) $Z_L=Z_{NE}=\infty, Z_s=Z_{FE}=50\ \Omega$;
(c) $Z_L=Z_{FE}=0, Z_s=Z_{NE}=50\ \Omega$;
(d) $Z_L=Z_{NE}=0, Z_s=Z_{FE}=50\ \Omega$.

load on the coupled I/O line. The geometry of the EMI antenna is shown in Figure 7, with the source representation being schematic only. A worst-case estimate of the antenna input impedance was needed for EMI calculations.
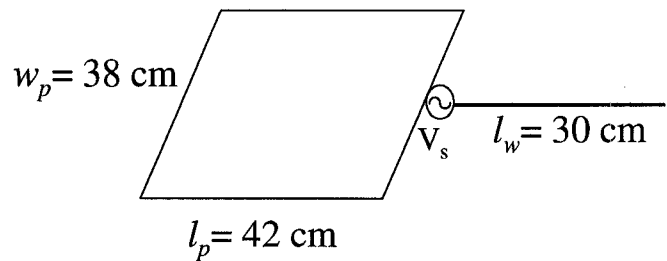

Figure 7. The geometry of the dipole-type EMI antenna.

A test geometry was constructed using the 38 cm × 42 cm PCB used in the previous coupling experiments. The test configuration (shown in Figure 8) was designed to place the effective antenna terminals at the edge of the PCB. A 0.085" coaxial semi-rigid cable was layed across the middle of the PCB with an SMA-connector on one side. The outer shield was terminated on the opposite side of the PCB, and the center conductor extended 30 cm beyond the board edge. The semi-rigid cable outer shield was soldered to a PCB ground (Layer 2) through vias distributed at locations along the cable shield.
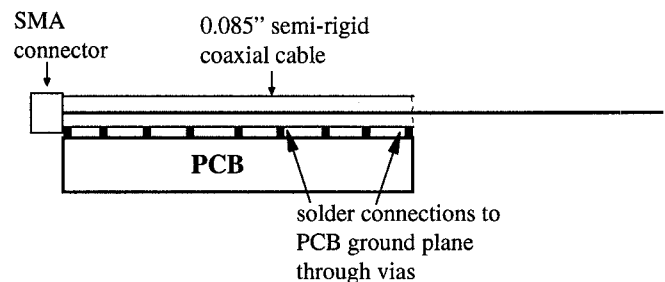

Figure 8. Test configuration for the dipole-type antenna impedance measurement.

The impedance was measured with an HP4291A impedance analyzer. In addition to measurements, the impedance of the described EMI antenna was also computed using the Finite-Difference Time-Domain (FDTD) method. A comparison of the measured and simulated results is shown in Figure 9. Although there is a discrepancy in particular in the resonance frequencies between the simulated and measured results, both results show that the impedance of the dipole-type antenna is around 70-90 Ω at odd-integer half wavelength resonance frequencies.

The common-mode current on a cable and EMI can be estimated for coupling from a high-speed digital signal to an I/O trace by modeling the coupling between the digital and I/O lines using the lumped-element sections, and using the antenna impedance to terminate the I/O line at the connector. A worst-case estimate is to assume the cable is driven as a resonant half wavelength antenna and ignore the signal load. The common-
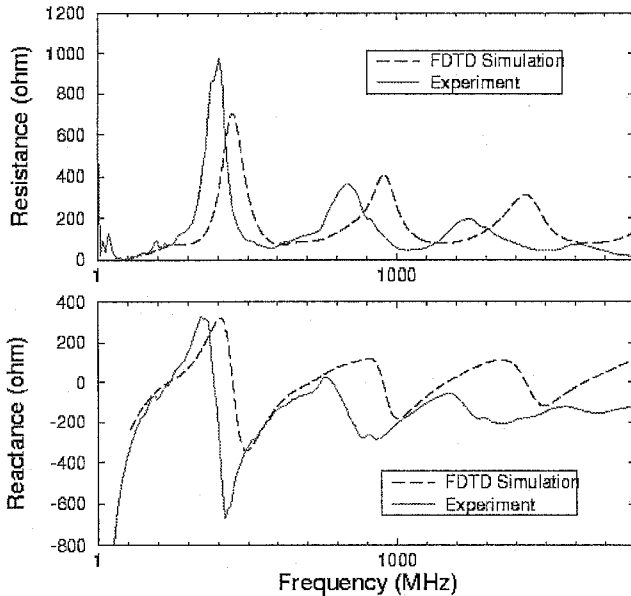
Figure 9. Experimental and simulated results of the input impedance for the antenna in Figure 8.

mode current and radiation due to the coupling between two microstrip lines were estimated for the previously studied geometry shown in Figure 5. The line was driven with a 5 V, 100 MHz, 1 ns rise-time trapezoidal signal with 50% duty-cycle. The source impedance was 50 Ω. The I/O line (far-end) was terminated in 70 Ω for a worst-case EMI estimate of the antenna input impedance. The coupled length of the two lines was 3 cm, and both the load of the driven line and near-end load of the coupled line were terminated in 50 Ω. The radiated field at 3 m (FCC Class B) was estimated simply with the field maximum for a half-wavelength dipole as [4]

$$|\vec{E}|_{max} = \frac{60 \, |I_{CM}|}{r} . \tag{10}$$

While this is a far-field approximation, it is a reasonable EMI approximation at 100 MHz, since the field is dominated by this term, even for kr~1 [8]. The estimated common-mode current and the electric field at 3m are (68.3μA, 63 dBμV/m), (63.6 μA, 62 dBμV/m), and (12.2 μA, 48 dBμV/m) at 100, 500 and 1100 MHz, respectively. Although the coupled length is only 3 cm, the calculated radiation from the driven cable was as high as 63 dBμV/m at 100 MHz. The calculated worst-case estimate exceeds FCC Class B limits by 20 dB at 100 MHz. While the 100 MHz trapezoidal signal is 5 V, and the 8 mil. wide traces are separated by only 5 mils., the estimate appears severe in the absence of supporting radiated EMI measurements. Among the shortcomings of the model, which may contribute to an over-estimate of the radiation, is that the signal return path, which is effectively in parallel with the EMI antenna, is not modeled. Also, a 70 Ω input impedance of the antenna being driven by the I/O line was assumed. While this is a worst-case scenario, the likelihood of it happening at every harmonic is not high. In addition, no filtering was added.

Further work is necessary in improving and experimentally corroborating the estimate.

VI. CONCLUSION

A lumped-element section model for coupling between PCB traces has been demonstrated experimentally for two extremes of loading conditions. This model was used together with an antenna model of a cable driven against a PCB ground plane for a worst-case EMI estimate. The results indicated that even very short parallel segments of a high-speed digital line tightly coupled to an I/O line can result in significant common-mode current and EMI.

REFERENCES

[1] C. R. Paul, "Decoupling the multiconductor transmission lines equations," *IEEE Trans. on Microwave Theory and Tech.*, vol. 44, no. 8, pp. 1429 - 1440, August 1996.

[2] J. S. Roychowdhury and D. O. Perderson, "Efficient transient simulation of lossy interconnect," *28th ACM/IEEE Design Automation Conference*, pp. 740-745, 1991.

[3] T. Dhaene and D. D. Zutter, "Selection of lumped element models for coupled lossy transmission lines," *IEEE Trans. on Computer-Aided Design*, vol. 11, no. 7, pp. 805-815, July 1992.

[4] C. R. Paul, *Introduction to Electromagnetic Compatibility*, New York: John Wiley & Sons, Inc., 1992.

[5] C. R. Paul, *Analysis of Multiconductor Transmission Lines*, New York: John Wiley & Sons, Inc., 1994.

[6] K. C. Gupta et. al., *Computer-Aided Design of Microwave Circuits*, Dedham, MA: Artech House, 1981.

[7] K. C. Gupta et. al., *Microstrip Lines and Slotlines*, Boston, MA: Artech House, 1996.

[8] C.A. Balanis, *Antenna Theory: Analysis and Design*, New York: John Wiley, 1997.